Energy and Enstrophy Cascades in Numerical Models

John Thuburn, James Kent and Nigel Wood

University of Exeter, Exeter,
EX4 4QF, United Kingdom
j.thuburn@ex.ac.uk

University of Michigan,
MI 48109-2143, USA
jdkent@umich.edu

Met Office, Exeter,
EX1 3PB, United Kingdom
nigel.wood@metoffice.gov.uk

ABSTRACT

The nonlinearity of the equations governing atmospheric flow implies interscale transfers of energy and potential enstrophy. It is important to understand how accurately these transfers are captured in numerical models, which have finite resolution and truncation errors, especially near the resolution limit, in the presence of scale-selective dissipation or other forms of subgrid model.

For the barotropic vorticity equation, energy and enstrophy transfers in spectral space due to truncated scales are calculated for a high resolution reference solution and for several explicit and implicit subgrid models. The reference solution shows a distinct and robust signal in which enstrophy and energy are removed from scales very close to the truncation limit and energy is transferred (backscattered) into those scales that are already most energetic. The subgrid models are able to capture the removal of enstrophy from small scales, though none are scale-selective enough. None of the subgrid models accurately captures the energy backscatter.

1   Introduction

In the absence of diabatic heating and frictional effects, the governing equations for atmospheric flow imply flux-form conservation laws for energy and potential enstrophy. Thus, energy and potential enstrophy are conserved both locally and globally. However, the nonlinearity of the flow leads to systematic transfers of energy and potential enstrophy between scales. In particular, there will be transfers between those scales that are resolvable and those that are unresolvable for any given finite-resolution numerical model. An important question, therefore, is: 'How well are the interscale transfers handled in weather forecast and climate models, particularly near the truncation limit?'

In this note we begin to address this question using the barotropic vorticity equation as a model problem. For the barotropic vorticity equation the conserved potential enstrophy simplifies to the enstrophy. We use a high-resolution reference solution to calculate directly the effect of scales smaller than some specified cut-off on the spectral tendencies of energy and enstrophy. These results are then compared with the spectral energy and enstrophy tendencies for a variety of explicit and implicit subgrid models when the data are truncated at the specified cut-off scale.

2   The need to remove potential enstrophy

It is well known that in two-dimensional turbulence and layer-wise two-dimensional quasi-geostrophic turbulence there is a systematic downscale cascade of potential enstrophy (e.g. Salmon 1998). If a numerical model captures this downscale cascade but conserves the *resolved* potential enstrophy, then potential enstrophy must accumulate near the truncation limit, a phenomenon called 'spectral blocking', leading to a noisy solution. Figure 1 illustrates this spectral blocking. The barotropic vorticity equation

$$\frac{\partial \zeta}{\partial t} + \nabla \cdot (\mathbf{v}\zeta) = 0, \quad \mathbf{v} = \nabla^{\perp}\psi, \quad \nabla^2 \psi = \zeta, \tag{1}$$
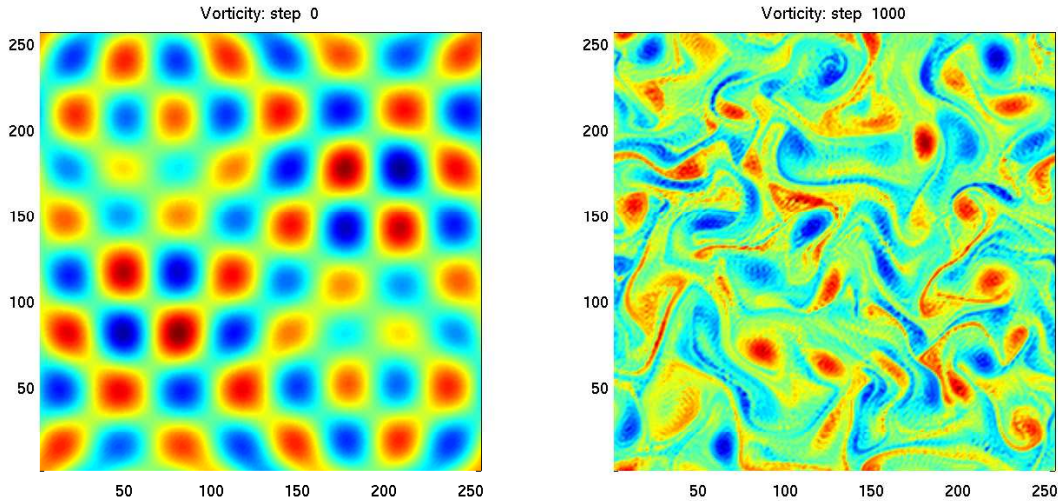
Figure 1: Initial vorticity (left) and vorticity after a few eddy turnover times (right) for a spectral solution of the barotropic vorticity equation with no explicit dissipation term. Red indicates positive vorticity, and blue indicates negative. The grid resolution is 256×256 and the spectral truncation is 85×85.

where ζ is vorticity, $\mathbf{v}$ is velocity, and ψ is stream function, is solved on a doubly periodic domain using a Fourier spectral method which, in the absence of any explicit dissipation terms, conserves both the energy

$$E = -\frac{1}{2} \int \psi \zeta \, dA \tag{2}$$

and the enstrophy

$$Z = \frac{1}{2} \int \zeta^2 \, dA. \tag{3}$$

The initial state is a not-quite-uniform array of vortices. After just a few eddy turnover times the solution has become noisy at the grid scale, and the noise becomes progressively worse as time increases.

Spectral blocking clearly points to the need for models to remove potential enstrophy near the truncation limit. In practice all models include some form of explicit or implicit scale-selective dissipation (e.g. Jablonowski and Williamson 2011), one of whose roles is to remove potential enstrophy.

However, a by-product of removing potential enstrophy is that energy is also removed. In the context of the barotropic vorticity equation, if enstrophy is removed at wavenumber k_{diss} at a rate $\dot{Z}$ then energy is also removed at a rate $\dot{E} = \dot{Z}/k_{\mathrm{diss}}^2$, and this latter quantity is bounded below by $\dot{Z}/k_{\mathrm{max}}^2$, where k_{max} is the maximum resolvable wavenumber. In practice energy and enstrophy are removed over a wide range of wavenumbers, so the ratio $\dot{E}/\dot{Z}$ is typically much greater than $1/k_{\mathrm{max}}^2$.

Estimates of the enstrophy and available energy budgets for the troposphere (Koshyk and Boer 1995, Thuburn 2008 and references therein) suggest enstrophy and energy throughputs $\dot{Z} \sim -10^{-15}\,\mathrm{s}^{-3}$ and $\dot{E} \sim -10^{-5}\,\mathrm{m}^{-2}\mathrm{s}^{-3}$ associated with nonlinear downscale cascades in the free atmosphere. (A much larger energy sink of order $\dot{E} \sim -10^{-4}\,\mathrm{m}^{-2}\mathrm{s}^{-3}$ is associated with boundary layer dissipation.) These numbers suggest that the required average dissipation scale is $k_{\mathrm{diss}} \sim 10^{-5}\,\mathrm{m}^{-1}$. There is evidence in the literature (e.g. Shutts 2005, Bowler et al. 2009), as well as much anecdotal evidence (e.g. WGNE 2003) that, at current climate resolutions and even resolutions used for ensemble weather prediction, state of the art models dissipate too much energy in the free atmosphere, perhaps by an order of magnitude. This can lead to insufficient variability and underdispersive ensembles.

One way to balance both the enstrophy and energy budgets in low resolution models is to feed some energy back in at larger scales. Diagnostics based on atmospheric analyses (Koshyk and Boer 1995) show that small scales do indeed mediate an energy transfer into large scales. There have been various proposals for representing this 'backscatter', including antidissipation at certain wavenumbers (Koshyk and Boer 1995), the Anticipated Potential Vorticity Method (Sadourny and Basdevant 1985), Stochastic Backscatter (e.g. Bowler et al. 2009), and vorticity confinement (e.g. Shutts, this volume).

3   Explicit and implicit subgrid models

The nonlinear effects of unresolved scales on resolved scales may be non-negligible, and therefore they need to be represented in numerical models. Formally this may be expressed using a filtered form of the governing equations (using the barotropic vorticity equation for illustration):

$$\frac{\partial \bar{\zeta}}{\partial t} + \nabla.(\bar{\mathbf{v}}\bar{\zeta}) = \text{SG}, \tag{4}$$

where

$$\text{SG} = \nabla.(\bar{\mathbf{v}}\bar{\zeta}) - \nabla.(\overline{\mathbf{v}\zeta}) \tag{5}$$

is the subgrid term and an overbar represents a filter that removes scales smaller than the model resolution.

Transfers of energy and potential enstrophy between resolved scales and unresolved scales are mediated by the unresolved scales. Therefore, the representation of these transfers is intimately related to the representation of the subgrid term SG.

Broadly, there are two approaches to representing the subgrid term. The explicit approach explicitly constructs a mathematical model for SG in terms of resolved variables and adds this to the right hand side of the discretized equations. The simplest example is a scale-selective hyperdiffusion of the form $K\nabla^{2n}$, but a range of more sophisticated schemes have been proposed (e.g. Smagorinsky 1963, Sadourny and Basdevant 1985, Frederiksen and Kepert 2006, Sagaut 2001, and references therein).

The alternative approach is known as Implicit Large-Eddy Simulation (ILES). In this approach the intention is to use a discretization of the governing equations whose truncation errors are able to play the role of a subgrid model. This approach is made plausible by noting that high-order upwind schemes with flux-limiters typically have truncation errors that take the form of a nonlinear scale-selective dissipation whose strength adapts to the strain rate of the resolved flow; these characteristics resemble those of many physically based subgrid models (Grinstein et al. 2007b).

There have been a number of studies of the validity of ILES for three-dimensional turbulence (e.g. Margolin and Rider 2002, 2007, Grinstein and Fureby 2006, Grinstein et al. 2007a), and some success has been claimed, though it appears less successful when upscale effects are important, for example near walls (Brown et al. 2000).

The layerwise two-dimensional turbulence of large-scale atmospheric flow is a rather different flow regime, and it is not clear that the success of ILES for three-dimensional flow will carry over. In layerwise-two-dimensional flow energy transfers are predominantly upscale (e.g. Salmon 1998), suggesting that ILES may be less successful. On the other hand, the energy spectrum is typically much steeper, suggesting a stronger slaving of small scales to large scales and therefore a greater possibility of representing the effects of small scales in terms of large scales. The issue is relevant to state-of-the-art weather and climate models using semi-Lagrangian advection schemes, since the interpolation errors introduce a scale-selective dissipation, meaning that in effect these models use the ILES approach.

Kent et al. (2011) studied the applicability of ILES to two-dimensional flow. Using the barotropic vorticity equation as a model problem, they diagnosed the cumulative effect of truncation errors on
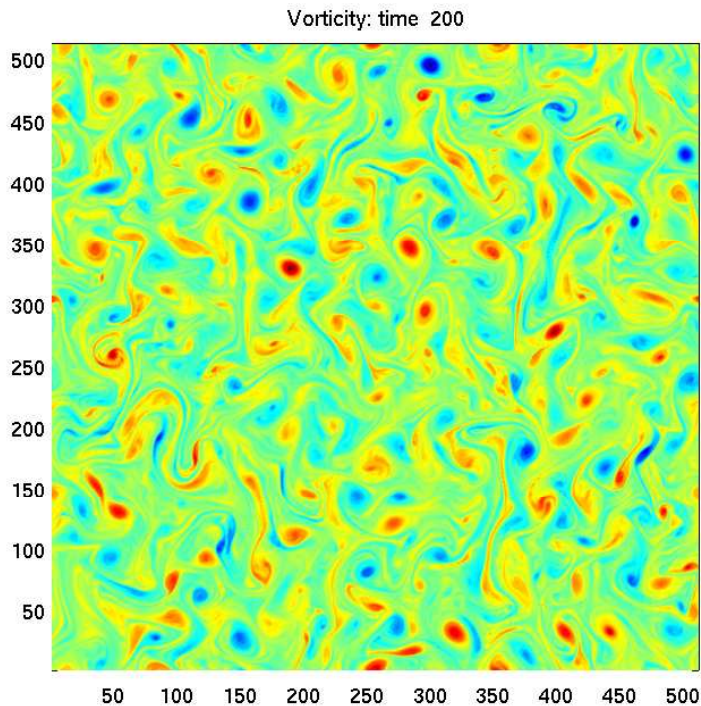
Figure 2: Vorticity at time $t = 200$ for a spectral solution of the barotropic vorticity equation with forcing and dissipation. Red indicates positive vorticity, and blue indicates negative. The grid resolution is 512×512 and the spectral truncation is 170×170.

the vorticity field for a variety of numerical schemes and compared them with the cumulative effect of the subgrid term diagnosed directly from a high-resolution reference solution. They found that several schemes, with both implicit and explicit subgrid models, could capture the leading order effects of the subgrid term when those effects were dissipative, for example when vorticity filaments were stretched and thinned to the resolution limit. However, none of the schemes was successful when the subgrid term involved upscale effects such as vortex merger or roll-up of thin vorticity filaments.

4 Effects on enstrophy and energy spectra of unresolved scales: direct calculation

In this section we use a high-resolution reference solution of the barotropic vorticity equation to diagnose the effects on the energy and enstrophy spectra of scales smaller than some specified cut-off. The calculation uses a doubly periodic domain discretized using a spectral numerical method truncated at maximum wavenumber 170×170; the transform grid has resolution 512×512 to avoid aliasing of quadratic terms. The flow is initialized from a higher resolution version of the initial state shown in Fig. 1; it is forced at wavenumber 16 and there is scale-selective ∇^8 dissipation term to remove enstrophy near the truncation limit and a scale-independent dissipation term ('Rayleigh friction') to remove energy on large scales. Figure 2 shows the vorticity field at time $t = 200$. (A typical peak vorticity value is of order 1, so one time unit is roughly one eddy turnover time.) At this time the flow is close to statistically steady. All the diagnostics presented below are for the instantaneous fields at this time.

The spectral energy and enstrophy tendencies due to small scales are calculated as follows. Assume we

know the Fourier transforms of the vorticity $\hat{\zeta}(\mathbf{k})$ and the stream function $\hat{\psi}(\mathbf{k}) = -\hat{\zeta}(\mathbf{k})/|\mathbf{k}|^2$, where $\mathbf{k}$ is the wavenumber. First the energy and enstrophy tendency at every wavenumber are calculated for the full-resolution data. This is done by transforming ζ and ψ and their spatial derivatives to grid space, calculating the Jacobian

$$J(\mathbf{x}) = \nabla.(\mathbf{v}\zeta) = \frac{\partial \psi}{\partial x}\frac{\partial \zeta}{\partial y} - \frac{\partial \psi}{\partial y}\frac{\partial \zeta}{\partial x} \tag{6}$$

on the transform grid and transforming back to spectral space to obtain $\hat{J}(\mathbf{k})$, ($\hat{J}$ is truncated to the maximum retained wavenumber, 170×170 in our example, to avoid aliasing), then computing

$$\dot{E}(\mathbf{k}) = Re\left\{\frac{\hat{\psi}^*(\mathbf{k})\hat{J}(\mathbf{k})}{\Delta k^2 N^4}\right\} \tag{7}$$

$$\dot{Z}(\mathbf{k}) = -Re\left\{\frac{\hat{\zeta}^*(\mathbf{k})\hat{J}(\mathbf{k})}{\Delta k^2 N^4}\right\}, \tag{8}$$

and finally integrating over angle in spectral space to obtain $\dot{E}(k)$ and $\dot{Z}(k)$. Here the superscript $*$ indicates a complex conjugate, $k = |\mathbf{k}|$, N is the grid resolution (512 in our example), Δk is the wavenumber interval in spectral space, and the factor $\Delta k^2 N^4$ arises from the normalization of the Fourier transforms. Second, the $\hat{\zeta}$ and $\hat{\psi}$ data are truncated to retain only those spectral components with $k < k_T$ for some truncation wavenumber k_T, and the calculation of the spectral energy and enstrophy tendencies is repeated to give $\dot{E}_T(k)$ and $\dot{Z}_T(k)$. Finally, the contribution mediated by wavenumbers greater than or equal to k_T is given by

$$\dot{E}_{SG}(k) = \dot{E}(k) - \dot{E}_T(k), \tag{9}$$

$$\dot{Z}_{SG}(k) = \dot{Z}(k) - \dot{Z}_T(k). \tag{10}$$

Figure 3 shows the results of this calculation for three different truncation wavenumbers: $k_T = 48, 96, 144$. The three $\dot{Z}_{SG}$ plots show that the truncated scales remove enstrophy from $k < k_T$ and transfer it to $k > k_T$. The scales from which enstrophy is removed are strongly localized close to k_T. The magnitude of the signal decreases as k_T increases, but the qualitative picture remains unchanged.

The three $\dot{E}_{SG}$ plots show that the truncated scales also remove energy from wavenumbers close to, but smaller than, k_T. However, they also transfer energy to large scales, to those wavenumbers that are already most energetic. This is the signal of energy backscatter. Again, the magnitude of the signal decreases as k_T increases, but the qualitative picture remains unchanged.

We have found this signal to be very robust. Repeating the calculation at other time instants produces almost identical plots to those shown. A qualitatively similar picture is seen even for rather idealized flows that are far from fully developed turbulence.

These results provide a reference solution against which to compare explicit or implicit subgrid models. Ideally, the subgrid model for a numerical solution with maximum resolved wavenumber k_T should be able to reproduce $\dot{E}_{SG}$ and $\dot{Z}_{SG}$ for the same k_T.

5 Effects on enstrophy and energy spectra of unresolved scales: explicit and implicit subgrid models

This section compares a number of explicit and implicit subgrid models against the reference solution found in section 4 in terms of their spectral energy and enstrophy transfers. In each case the data are truncated to wavenumber k_T before the chosen scheme is applied. For this comparison $k_T = 96$.

Figure 4 shows the spectral energy and enstrophy tendencies due to simple, explicit ∇^4 and ∇^8 hyperdiffusion subgrid models. A ∇^4 subgrid model removes enstrophy predominantly from large wavenumbers,
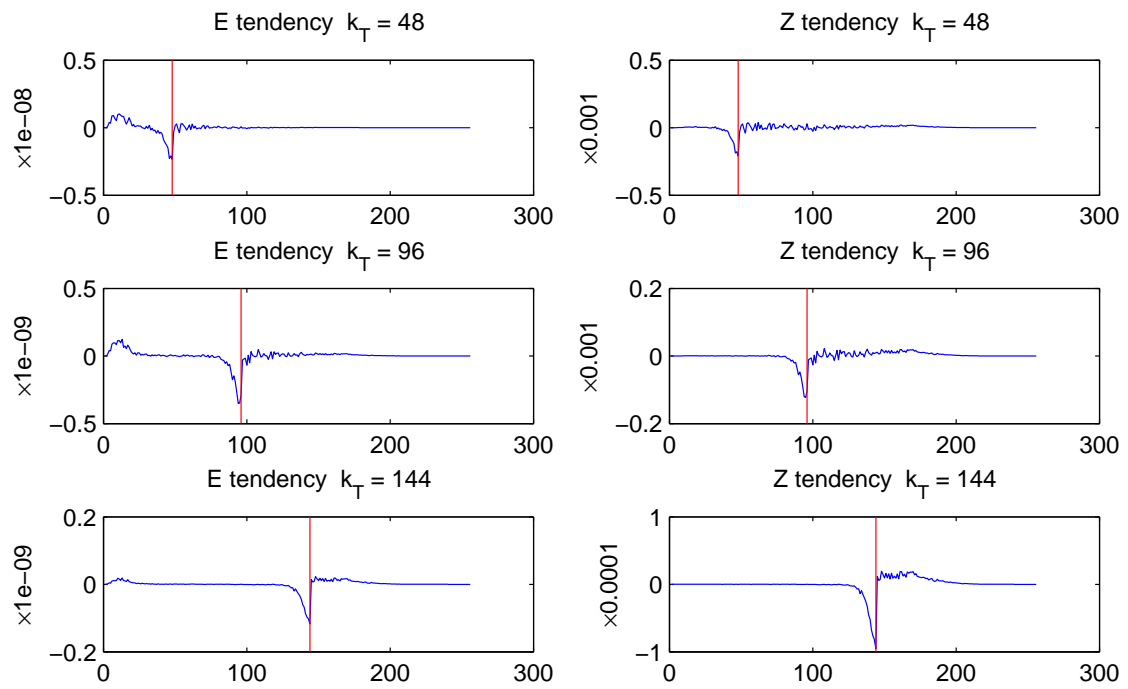
Figure 3: Spectral tendencies of energy $\dot{E}_{SG}(\mathbf{k})$ (left) and enstrophy $\dot{Z}_{SG}(\mathbf{k})$ (right) mediated by wavenumbers greater than or equal to k_T. Top: $k_T = 48$; middle $k_T = 96$; bottom: $k_T = 144$. Note the different axis scales for the different values of k_T.
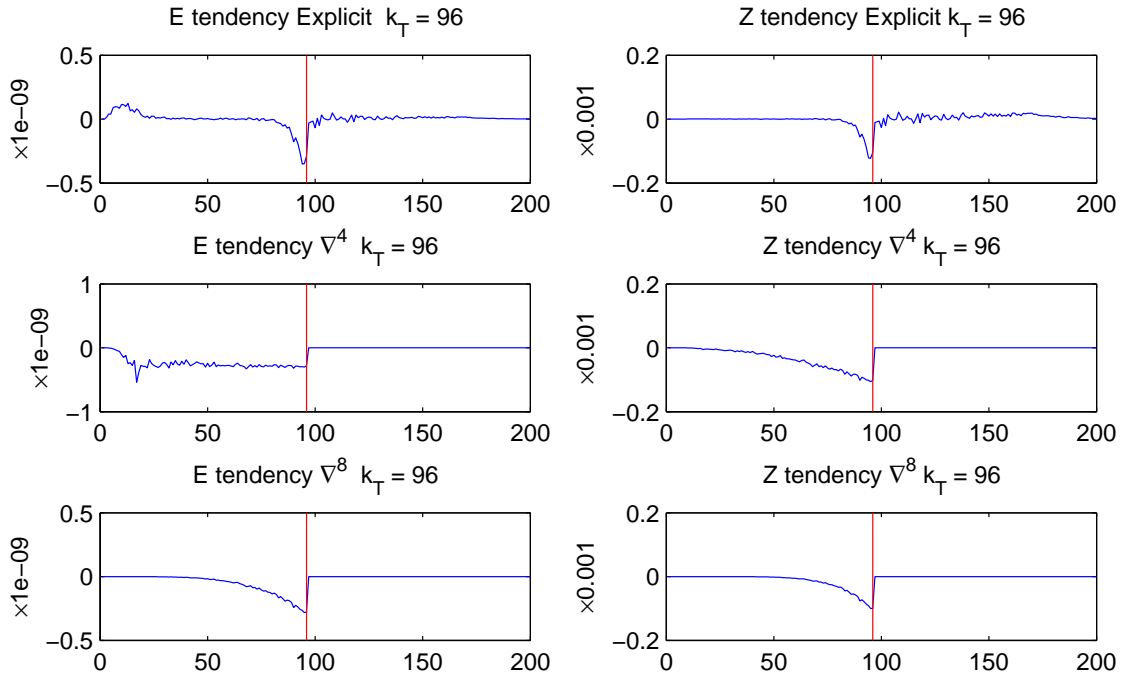
Figure 4: Top: $\dot{E}_{SG}(\mathbf{k})$ and $\dot{Z}_{SG}(\mathbf{k})$ for $k_T = 96$ (same as the middle row of Fig. 3). Middle: $\dot{E}_{SG}(\mathbf{k})$ and $\dot{Z}_{SG}(\mathbf{k})$ for a ∇^4 subgrid model. Bottom: $\dot{E}_{SG}(\mathbf{k})$ and $\dot{Z}_{SG}(\mathbf{k})$ for a ∇^8 subgrid model.

but is much less scale-selective than the reference solution. This is even more conspicuous in terms of spectral energy tendency, which is almost flat for wavenumbers greater than about 10. Importantly, energy is removed at all wavenumbers; there is no representation of the backscatter. A ∇^8 subgrid model is more scale-selective, but still significantly less so than the reference solution. Again, there is no representation of backscatter.

UTOPIA (Leonard et al. 1993) is a quasi-third-order upwind flux-form advection scheme (it becomes third order when the advecting velocity is constant). It has inherent scale-selective dissipation, and is therefore the type of scheme that might be suitable for ILES. It may be used with a flux limiter (Thuburn 1996) to prevent overshoots and undershoots. Figure 5 shows an estimate of the effect of truncation errors on the spectral energy and enstrophy tendencies when UTOPIA is used for advection of vorticity. The estimate is obtained by using the Jacobian implied by UTOPIA in (7) and (8) to obtain $\dot{E}_U, \dot{Z}_U$, then subtracting $\dot{E}_T$ and $\dot{Z}_T$, which are computed using the spectral scheme (which has no spatial truncation errors for the resolved scales).

The results show that UTOPIA's truncation errors do indeed remove enstrophy near the truncation limit, though it is not as scale selective as the reference solution. However, it also gives large enstrophy transfers at small wavenumbers, with both sources and sinks. The large enstrophy sources and sinks imply extremely large energy sources and sinks; they are two orders of magnitude larger than the reference solution backscatter signal. The inclusion of a flux limiter makes negligible difference to the results.

We speculate that the large energy sources and sinks at low wavenumber arise as follows. The high accuracy of the UTOPIA advection scheme is obtained through a cancellation of leading truncation errors in the numerical fluxes when their divergence is calculated. Because UTOPIA is an upwind scheme, there is a 'jump' in the stencil used to compute the fluxes at locations where one of the velocity components changes sign, at these locations the cancellation of leading truncation error no longer occurs
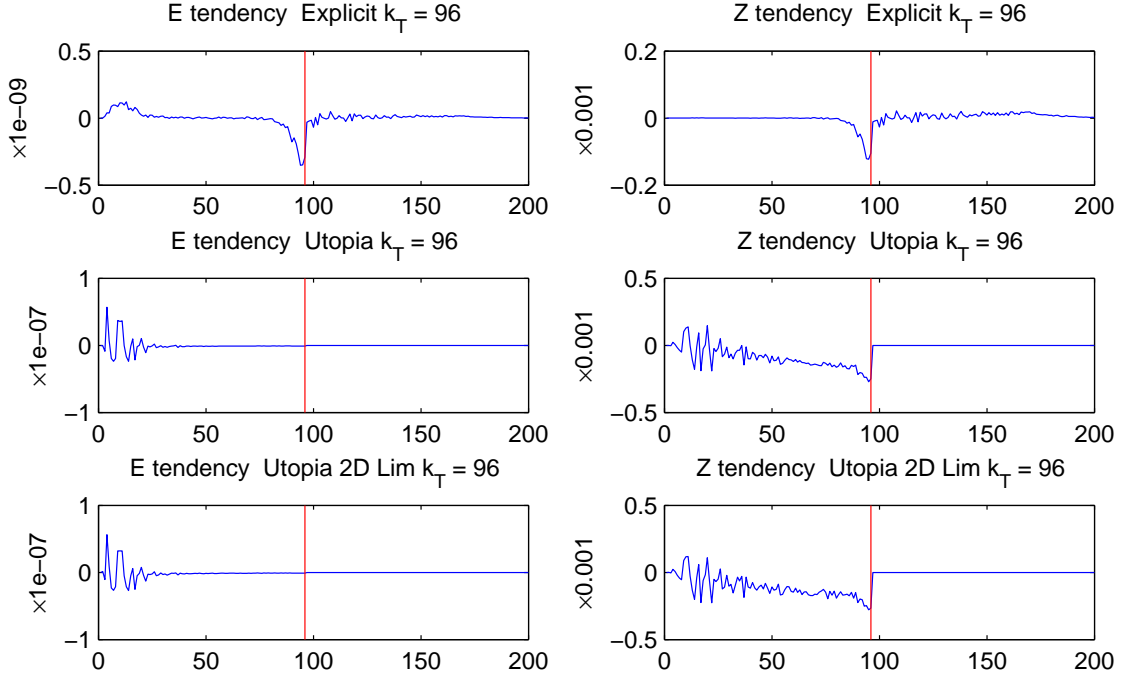
Figure 5: Top: $\dot{E}_{SG}(\mathbf{k})$ and $\dot{Z}_{SG}(\mathbf{k})$ for $k_T = 96$ (same as the middle row of Fig. 3). Middle: $\dot{E}_{SG}(\mathbf{k})$ and $\dot{Z}_{SG}(\mathbf{k})$ for the truncation errors of the UTOPIA scheme. Bottom: $\dot{E}_{SG}(\mathbf{k})$ and $\dot{Z}_{SG}(\mathbf{k})$ for the truncation errors of the flux-limited UTOPIA scheme.

and the accuracy is significantly reduced. Thus, the flow domain is criss-crossed by zones of relatively large error, and this pattern projects significantly onto low wavenumbers.

The Anticipated Potential Vorticity Method (APVM, Sadourny and Basdevant 1985) was proposed as a scheme for dissipating enstrophy while conserving energy in hydrostatic primitive equation atmospheric models. It takes the form of a modification to the Coriolis term in the momentum equation. When applied to the barotropic vorticity equation the scheme is

$$\frac{\partial \mathbf{v}}{\partial t} + (\zeta - D)\hat{\mathbf{k}} + \nabla \left(p + \frac{\mathbf{v}^2}{2} \right) = 0, \tag{11}$$

where $\hat{\mathbf{k}}$ is the unit vertical vector and p is the pressure, or in terms of the vorticity equation itself,

$$\frac{\partial \zeta}{\partial t} + \nabla.(\mathbf{v}\zeta) = \nabla.(\mathbf{v}D). \tag{12}$$

Here, $D = \theta \mathscr{L}(\mathbf{v}.\nabla \zeta)$ for some positive definite linear operator $\mathscr{L}$ and suitable tunable parameter θ. We consider two possibilities proposed by Sadourny and Basdevant (1985): $\mathscr{L} = 1$ implying

$$\dot{Z} = -\theta \int (\mathbf{v}.\nabla \zeta)^2 \, dA, \tag{13}$$

and $\mathscr{L} = -\nabla^2$ implying

$$\dot{Z} = -\theta \int (\nabla(\mathbf{v}.\nabla \zeta))^2 \, dA. \tag{14}$$
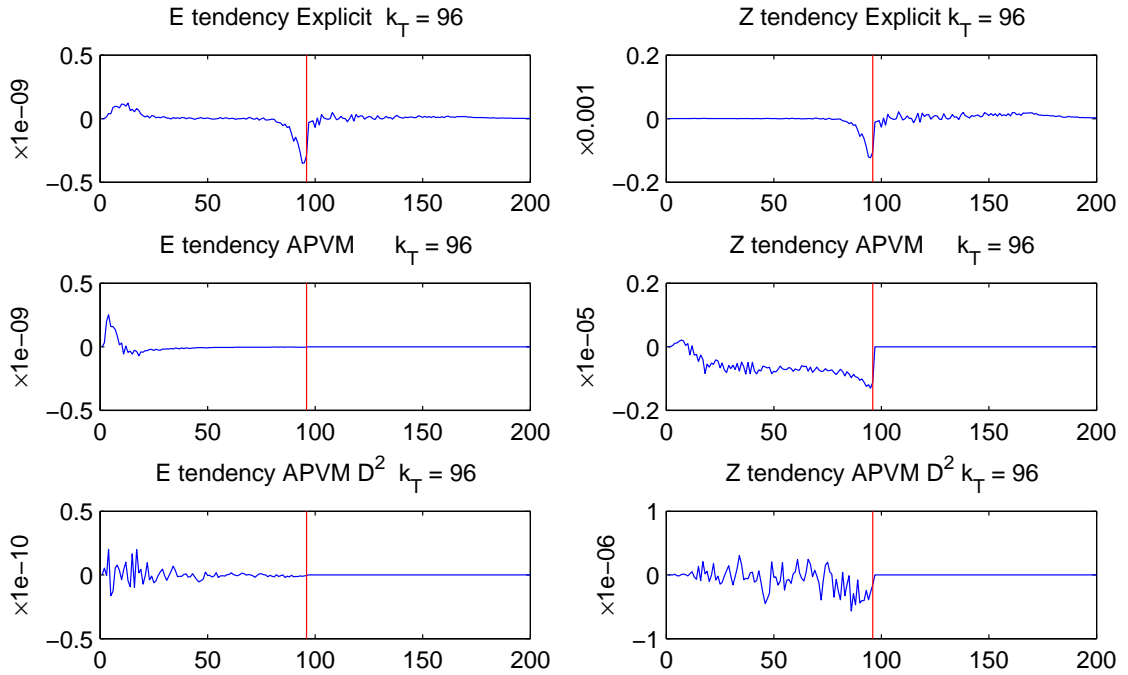
All terms are calculated using the spectral method.

Figure 6: Top: $\dot{E}_{\mathrm{SG}}(\mathbf{k})$ and $\dot{Z}_{\mathrm{SG}}(\mathbf{k})$ for $k_T = 96$ (same as the middle row of Fig. 3). Middle: $\dot{E}_{\mathrm{SG}}(\mathbf{k})$ and $\dot{Z}_{\mathrm{SG}}(\mathbf{k})$ for the $\mathscr{L} = 1$ APVM. scheme. Bottom: $\dot{E}_{\mathrm{SG}}(\mathbf{k})$ and $\dot{Z}_{\mathrm{SG}}(\mathbf{k})$ for the $\mathscr{L} = -\nabla^2$ APVM.

Figure 6 shows the spectral energy and enstrophy tendencies due to the APVM subgrid model $\nabla.(\mathbf{v}D)$. For the $\mathscr{L} = 1$ version of the scheme, there is indeed a net removal of enstrophy while the total energy is conserved. Consistent with this, there is a net upscale transfer of energy; however, this transfer is fairly local in wavenumber space, in contrast to the reference solution in which the energy transfer is very nonlocal. Although there is some preference for enstrophy removal to occur at the smallest scales, it is significant across most of the spectrum. Moreover, when the coefficient θ is tuned so that the peak energy source is comparable to the reference solution (as here), the enstrophy removal is much smaller than for the reference solution. The $\mathscr{L} = -\nabla^2$ version of the scheme again gives a net enstrophy sink while conserving energy, but the spectral distribution of sources and sinks is very erratic and very different from reference solution.

6 Conclusions

There is evidence that numerical models of the atmosphere dissipate too much energy in the free atmosphere, and this can lead to insufficient variability and underdispersive ensembles.

Using the barotropic vorticity equation as a model problem, we have examined the contribution to spectral energy and enstrophy tendencies due to subgrid scales, first by direct calculation using a high-resolution reference solution, then for several explicit and implicit subgrid models. The direct calculation shows a distinct and robust signal: enstrophy and energy are removed from scales very close to the truncation scale, and energy is transferred to those scales that are already most energetic.

All of the subgrid modes tested are able to remove enstrophy predominantly from the smallest resolved scales, though none are as scale-selective as the reference solution. None of the subgrid models tested

is able to capture a realistic energy backscatter signal. The $\mathscr{L} = 1$ version of APVM does provide an upscale energy transfer, but this is too local in wavenumber space. The other schemes either remove energy across too wide a range of scales, or produce large and unrealistic energy transfers at small wavenumbers.

The tendency of typical subgrid models to remove energy across too wide a range of scales is likely to be related to the excessive disspation reported in atmospheric models. The effect is systematic and deterministic, suggesting that a *deterministic* scheme to restore the missing energy might be appropriate. Kent (2009) tested a simple scheme for the barotropic vorticity equation, targeting energy input at intermediate wavenumbers; he was able to improve the energy budget and found a small but measurable improvement in the accuracy of the vorticity solution. Targeting energy input at small wavenumbers was less successful, implying that it is more important to repair the excessive numerical dissipation at intermediate scales than to capture the physical backscatter to large scales.

References

Bowler, N. E., A. Arribas, S. E. Beare, K. R. Mylne, G. J. Shutts (2009). The local ETKF and SKEB: Upgrades to the MOGREPS short-range ensemble prediction system. *Quart. J. Roy. Meteorol. Soc.*, **135**, 767-776.

Brown, A. R., M. K. MacVean, and P. J. Mason (2000). The effects of numerical disipation in large eddy simulations. *J. Atmos. Sci.*, **57**, 3337-3348.

Frederiksen, J. S. and S. M. Kepert (2006). Dynamical subgrid-scale parameterizations from direct numerical simulations. *J. Atmos. Sci.*, **63**, 3006-3019.

Grinstein, F. F. and C. Fureby (2006). Recent Progress on Flux-Limiting Based Implicit Large Eddy Simulation. *European Conference on Computational Fluid Dynamics, ECCOMAS CFD 2006*

Grinstein, F. F., L. G. Margolin, and W. J. Rider (2007a). Implicit Large Eddy Simulation. Cambridge University Press, 546 pp.

Grinstein, F. F., L. G. Margolin, and W. J. Rider (2007b). A rationale for implicit LES. In: Implicit Large-Eddy Simulation, Grinstein, F. F., Margolin, L. G. and Rider, W. J., Eds, Cambridge University Press, 546 pp.

Jablonowski, C. and D. L. Williamson (2011). The pros and cons of diffusion, filters and fixers in atmospheric general circulation models. In: Numerical Techniques for Global Atmospheric models, Lauritzen, P. H., Jablonowski, C., Taylor, M. A., and Nair, R. D., Eds, Springer, 556pp.

Kent, J. (2009). Assessing Implicit Large Eddy Simulation for two-dimensional flow. PhD Thesis, University of Exeter. https://eric.exeter.ac.uk/repository/handle/10036/91904

Kent, J., J. Thuburn, and N. Wood (2011). Assessing Implicit Large Eddy Simulation for two-dimensional flow. *Submitted to Quart. J. Roy. Meteorol. Soc.*

Koshyk, J. N. and G. J. Boer (1995). Parametrization of dynamical subgrid-scale processes in a spectral GCM. *J. Atmos. Sci.*, **52**, 965-976.

Leonard, B. P., M. K. MacVean, and A. P. Lock (1993). Positivity-Preserving Numerical Schemes for Multidimensional Advection. *NASA Technical Memorandum 106055*.

Margolin, L. G. and W. J. Rider (2002). A Rationale for Implicit Turbulence Modeling. *International Journal for Numerical Methods in Fluids*, **39**, 821-841. 2002

Margolin, L. G. and W. J. Rider (2007). Numerical regularization: The numerical analysis of implicit

subgrid models. In: Implicit Large-Eddy Simulation, Grinstein, F. F., Margolin, L. G. and Rider, W. J., Eds, Cambridge University Press, 546 pp.

Sadourny, R., and C. Basdevant (1985). Parameterization of subgrid scale barotropic and baroclinic eddies in quasi-geostrophic models: Anticipated potential vorticity method. *J. Atmos. Sci.*, **42**, 1353-1363.

Sagaut, P. (2001). Large Eddy Simulation for incompressible flows. Springer, 319pp.

Salmon, R. (1998). Lectures on Geophysical Fluid Dynamics, Oxford University Press, 378pp.

Shutts, G. (2005). A kinetic energy backscatter algorithm for use in ensemble prediction systems. *Quart. J. Roy. Meteorol. Soc.*, **131**, 3079-3102.

Smagorinsky, J. (1963). General circulation experiments with the primitive equations. I. The basic experiment. *Mon. Wea. Rev.*, **91**, 99-164.

Thuburn, J. (1996). Multidimensional Flux-Limited Advection Schemes. *Journal of Computational Physics*, **123**, 74-83.

Thuburn, J. (2008). Some conservation issues for the dynamical cores of NWP and climate models. *J. Comput. Phys.*, **227**, 3715-3730.

WGNE, (2003). WMO Atmospheric Research and Environment Programme, CAS/JSC Working Group on Numerical Experimentation, Report No. 18.

ECMWF Workshop on Model Uncertainty, 20 – 24 June 2011